JOURNAL OF CATALYSIS **169,** 263–274 (1997)
ARTICLE NO. CA971700

Iridium Clusters in KLTL Zeolite: Synthesis, Structural Characterization, and Catalysis of Toluene Hydrogenation and *n*-Hexane Dehydrocyclization

Ailian Zhao, R. E. Jentoft, and B. C. Gates[1]

Department of Chemical Engineering and Materials Science, University of California, Davis, California 95616

Received September 3, 1996; revised March 21, 1997; accepted March 24, 1997

Iridium clusters incorporating about six atoms each, on average, were prepared in KLTL zeolite by decarbonylation (in H_2 at 400°C) of iridium carbonyl clusters formed by treatment of adsorbed [$Ir(CO)_2$(acac)] in CO at 1 atm and 175°C. The supported species were characterized by infrared and extended X-ray absorption fine structure (EXAFS) spectroscopies. The iridium carbonyls formed from [$Ir(CO)_2$(acac)] were predominantly $[HIr_4(CO)_{11}]^-$ with a small amount of $[Ir(CO)_4]^-$. The synthesis chemistry of iridium carbonyls in the basic KLTL zeolite parallels that in basic solutions. Shifts of the ν_{CO} bands of the iridium carbonyl clusters relative to those of the same clusters in solution indicate strong interactions between the clusters and zeolite cations. The decarbonylated sample, approximated as Ir_6/KLTL zeolite, is catalytically active for toluene hydrogenation at 60–100°C, with the activity being approximately the same as those of Ir_4 and Ir_6 clusters supported on metal oxides, but an order of magnitude less than that of a conventional supported iridium catalyst consisting of aggregates of about 50 atoms each, on average. The catalyst is also active for conversion of *n*-hexane + H_2 at 340–420°C, but the selectivity for aromatization is low and that for hydrogenolysis is high, consistent with earlier results for conventionally prepared (salt-derived) iridium clusters of about the same size supported in KLTL zeolite. The zeolite-supported iridium clusters are the first prepared from both salt and organometallic precursors; the results indicate that the organometallic and conventional preparation routes lead to supported iridium clusters having similar structures and catalytic properties.

INTRODUCTION

Interest in zeolite-supported metals has been heightened by the discovery of highly selective alkane dehydrocyclization catalysts consisting of platinum clusters in zeolite LTL (1–3); these catalysts are made conventionally from salt precursors and applied industrially for naphtha conversion (4, 5). For years, researchers have found it difficult to determine the sizes of metal clusters and particles in and on zeolites, but recent work with Pt/LTL zeolites has shown that in well-prepared catalysts the platinum is present in the form of extremely small clusters, about 5–12 atoms each, on average (6–9), as shown by extended X-ray absorption fine structure (EXAFS) spectroscopy and transmission electron microscopy.

These clusters are so small as to be considered nearly molecular in nature. There are still only a few well-documented examples of such supported clusters, most of them prepared from molecular and ionic organometallic precursors, such as $[Ir_4(CO)_{12}]$ (10–12) and $[Ir_6(CO)_{15}]^{2-}$ (13, 14). These precursors on support surfaces have been decarbonylated with the cluster frames almost intact to give nearly uniform clusters, represented as Ir_4 and Ir_6, for example (9–14). Ir_6 in NaY zeolite has been reversibly recarbonylated, as indicated by infrared spectroscopy (15, 16). These results demonstrate connections between molecular and supported metal clusters (17) and suggest additional opportunities for preparation of supported metal clusters that are virtually molecular in character.

Almost all the supported metal clusters that have been characterized in some depth (which, to us, implies characterization by EXAFS spectroscopy) are iridium. Thus, to meet the goal of comparing supported metal cluster catalysts prepared from organometallic precursors with those prepared conventionally from salt precursors, we have investigated iridium clusters in KLTL zeolite. Catalysts prepared from salt precursors were reported recently (18, 19); catalysts prepared from organometallic precursors are reported here. The samples were characterized by infrared and EXAFS spectroscopies and tested as catalysts for toluene hydrogenation and *n*-hexane reforming.

EXPERIMENTAL METHODS

Materials

[$Ir(CO)_2$(acac)] [dicarbonyl(acetylacetonato)iridium(I), 99%, Strem] was used as received. KLTL zeolite (K : Al atomic ratio = 1.08, Union Carbide) from a batch that was

[1] To whom correspondence should be addressed.

0021-9517/97 $25.00

used in related work (18, 19) was washed with deionized water until the pH of the solution was about 9 and then dried at 120°C overnight. The zeolite was crushed into fine powder, calcined at 400°C, and placed in a Braun MB-150M N_2-filled glovebox. *n*-Hexane (>99% purity, Aldrich) and toluene (99.7%, J. T. Baker) were degassed by sparging of N_2 (99.997%, Liquid Carbonic) for 2 h before use. He (99.995%) and CO (CP grade, 99.5%) were supplied by Liquid Carbonic and passed through traps containing particles of Cu_2O and zeolite 4A to remove traces of O_2 and moisture. H_2 with a purity of 99.999% was generated by a Balston H_2 generator (Type 75-33) and passed through the same traps used for He.

Catalyst Preparation

Introduction of [Ir(CO)$_2$(acac)] into zeolite. The KLTL zeolite calcined at 400°C was brought into contact with [Ir(CO)$_2$(acac)] in degassed *n*-hexane in a Schlenk flask under N_2. The mixture was stirred for 2 days at room temperature and dried by evacuation for 8 h at room temperature. The iridium content of the solid was calculated to be 1 wt% on the basis of results indicating that the uptake was virtually complete during the adsorption.

Carbonylation. The KLTL zeolite-supported [Ir(CO)$_2$(acac)] was carbonylated by treatment in flowing CO in a tubular reactor at 175°C for 10 h to form iridium carbonyl clusters. The product was handled in the glovebox and characterized by infrared spectroscopy and X-ray absorption spectroscopy.

Decarbonylation. The KLTL zeolite containing iridium carbonyl clusters was treated in flowing H_2 at 400°C for 2 h to give decarbonylated iridium clusters supported in the zeolite. The decarbonylated sample was characterized by H_2 chemisorption and X-ray absorption spectroscopy.

Catalyst Characterization

H_2 chemisorption. H_2 chemisorption was carried out with an RXM-100 catalyst testing and characterization apparatus (Advanced Scientific Design, Inc.). About 200 mg of a sample incorporating iridium carbonyl clusters supported in KLTL zeolite was treated in H_2 at 400°C for 2 h followed by evacuation at pressures $\leq 10^{-7}$ Torr at 400°C for 2 h. The sample was cooled to room temperature under vacuum before the chemisorption experiments were carried out. Adsorption isotherms were measured at 25°C and pressures between 10 and 200 Torr. After the first isotherm (representing chemisorption and physisorption) had been measured, the sample was evacuated for 30 min at 25°C, and the measurement of the second isotherm (measuring only physisorption) was carried out. The difference between the two isotherms represents the amount of H_2 irreversibly chemisorbed on iridium.

X-ray absorption spectroscopy. The X-ray absorption experiments were performed on beamline 2-3 at the Stanford Synchrotron Radiation Laboratory (SSRL) at the Stanford Linear Accelerator Center, Stanford, California. The storage ring operated with an electron energy of 3 GeV, and the beam current was 40–100 mA.

Wafers of sample for the transmission X-ray absorption spectroscopy experiments were prepared in a N_2-filled glovebox (Vacuum Atmospheres) at the Synchrotron. The wafers were prepared as follows: Each powder sample was placed in a holder in the glovebox. The holder was placed in a pressing die, and the sample was pressed into a self-supporting wafer. After pressing, the sample in the holder was mounted in a transmission EXAFS cell, described elsewhere (20), and sealed.

Each sample was either scanned as is or treated in H_2 at 400°C for 2 h before scanning. X-ray absorption data were recorded with the sample under vacuum at approximately liquid nitrogen temperature. Higher harmonics in the X-ray beam were minimized by detuning the Si(220) double-crystal monochromator by 15–20% at the iridium L_{III} absorption edge (11215 eV).

Precautions were taken to allow transport of the samples to SSRL without air contamination. Each sample was placed inside double layers of glass vials, each individually sealed with a vial cap and Parafilm.

EXAFS reference data. The EXAFS data were analyzed with experimentally determined reference files obtained from EXAFS data for materials of known structure. Details are given elsewhere (14). The parameters used to extract these files from the EXAFS data are summarized in Table 1.

Catalytic Reactions Catalyzed by KLTL Zeolite-Supported Iridium Clusters

Toluene hydrogenation. Toluene hydrogenation catalyzed by KLTL zeolite-supported iridium clusters was carried out in a tubular flow reactor packed with catalyst powder. The catalyst was pretreated *in situ* prior to the rate measurements. Typically, 80 mg of catalyst sample consisting of KLTL zeolite-supported iridium carbonyl clusters was mixed with 800 mg of inert α-Al_2O_3 powder and loaded into a Pyrex reactor to give a catalyst bed about 5 mm deep. The supported iridium carbonyl precursors were decarbonylated in flowing H_2 at 400°C for 2 h to form supported iridium clusters, followed by purging with He at 400°C for 0.5 h.

In a catalysis experiment, toluene was injected into the flow system at a constant rate by an Isco liquid metering pump (Model 260D), flowing to a vaporizer held at about 120°C. The reaction mixture consisted of H_2 and vaporized toluene, which passed at atmospheric pressure through the reactor at a total flow rate of 46 ml(NTP)/min.

TABLE 1

Structural Parameters Characterizing Reference Compounds and the Fourier Transform Ranges Used for Preparation of the Reference Files

Reference compound	Crystallographic data				Fourier transform[a]		
	Shell	N	r (Å)	Ref.	Δk (Å^{-1})	Δr (Å)	n
Pt foil	Pt–Pt	12	2.77	(21)	1.9–19.8	1.9–3.0	3
$Na_2Pt(OH)_6$	Pt–O	6	2.05	(22)	1.4–17.7	0.5–2.0	3
$[Ir_4(CO)_{12}]$	Ir–C	3	1.87	(23)	2.8–16.5	1.1–2.0	3
	Ir–O*	3	3.01	(23)	2.8–16.5	2.0–3.3	3
IrAl alloy	Ir–Al[b]	8	2.58	(12)	2.7–12.0[c]	0.98–2.98	3

[a] Notation: N, coordination number; Δk, limits of forward Fourier transformation (k is the wavevector); Δr, limits of shell isolation (r is the absorber–backscatterer distance); n, power of k used for Fourier transformation. O* is carbonyl oxygen.

[b] After subtraction of Ir–Ir contribution: $N = 6$, $r = 2.98$ Å, Debye–Waller factor $\Delta\sigma^2 = -0.001$ Å^2, inner potential correction $\Delta E_0 = -3.3$ eV (12).

[c] Assuming that M was Al, a theoretical Ir–Al EXAFS function was calculated with the FEFF4 program (24) and adjusted to agree with the limited Ir–Al reference data obtained as described here for use of a larger interval in k space for fitting the iridium data (12); however, M cannot be identified with confidence, and the results given here are only illustrative.

The reactor was mounted in an electrically heated and temperature-controlled Lindberg furnace. The effluent gas mixture was analyzed with an on-line Hewlett–Packard gas chromatograph (HP-5890 Series II) equipped with a DB-624 capillary column (J&W Scientific) and a flame ionization detector. The catalytic activity was measured under the following conditions: partial pressures $P_{H_2} = 710$ Torr and $P_{toluene} = 50$ Torr; temperature = 60, 80, or 100°C.

n-Hexane conversion with H_2. Reforming of *n*-hexane to give benzene catalyzed by KLTL zeolite-supported iridium clusters was performed in an apparatus similar to that used for toluene hydrogenation. The powder catalyst sample (200 mg) consisting of KLTL zeolite-supported iridium carbonyl clusters was mixed with 800 mg of α-Al_2O_3 and loaded into a tubular stainless-steel reactor and treated in flowing H_2 at 400°C for 2 h to form decarbonylated iridium clusters on the support. The catalyst was cooled to the reaction temperature in flowing H_2. Vaporized *n*-hexane was mixed with H_2 prior to passing through the catalyst bed. The gas mixture at 1 atm flowed at a total rate of 22 ml(NTP)/min, with the molar ratio of H_2 to *n*-hexane being 7. The conversion of *n*-hexane was measured at 340, 380, and 420°C.

RESULTS

Characterization of Iridium Carbonyl Clusters Supported in KLTL Zeolite

Infrared spectroscopy. The solid formed by adsorbing $[Ir(CO)_2(acac)]$ in KLTL zeolite that had been calcined at 400°C was beige in color after removal of the solvent, with the ν_{CO} infrared spectrum 2087 sh, 2063 s, 1979 s, 1955 sh cm^{-1} and an unidentified band at 1776 m cm^{-1} (Fig. 1). The ν_{CO} bands at 2063 and 1979 cm^{-1} indicate iridium dicarbonyls (25); thus, the adsorbed mononuclear iridium species is formulated as $[Ir(I)(CO)_2]$/KLTL. The band at 1776 cm^{-1} is characteristic of the KLTL zeolite itself, appearing in the spectrum of KLTL zeolite before adsorption of $[Ir(CO)_2(acac)]$.

Treatment of the zeolite-supported iridium dicarbonyl in CO at 175°C for 10 h led to an infrared spectrum (ν_{CO}: 2093 m, 2063 s, 2037 m, 2011 m, 1985 m, 1941 m, 1920 s, 1732 m, 1708 m cm^{-1}, Fig. 2) suggesting the formation of a mixture of iridium carbonyls. Part of this spectrum (2093, 2063, 2037, 1732, and 1708 cm^{-1}) resembles the ν_{CO} spectrum of $[PPN][HIr_4(CO)_{11}]$ [PPN is bis(triphenylphosphine)nitrogen(1+)] in CH_3OH (25) and that reported for $[HIr_4(CO)_{11}]^-$ supported on partially dehydroxylated MgO (10) (Table 2); however, the terminal ν_{CO} bands are shifted to higher frequencies and the bridging ν_{CO} bands to lower frequencies relative to those of $[HIr_4(CO)_{11}]^-$. The strong ν_{CO} band at 1920 cm^{-1} is attributed to $[Ir(CO)_4]^-$ (25, 26); the terminal ν_{CO} band is shifted to a higher frequency relative to that of $[Ir(CO)_4]^-$ in solution (Table 2). The other (weak) ν_{CO} bands in Fig. 2 are not assigned; they may be minor bands of

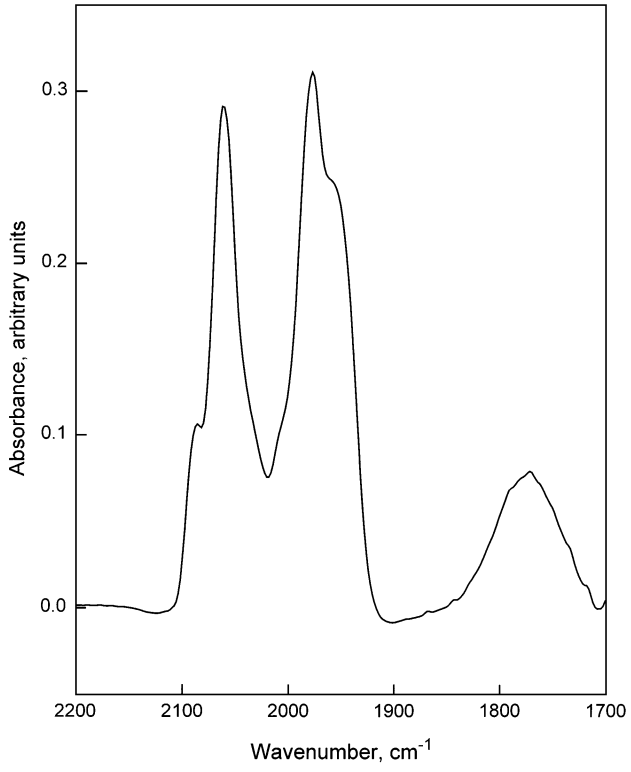

FIG. 1. Infrared spectrum of the species prepared by adsorption of $[Ir(CO)_2(acac)]$ in KLTL zeolite calcined at 400°C.

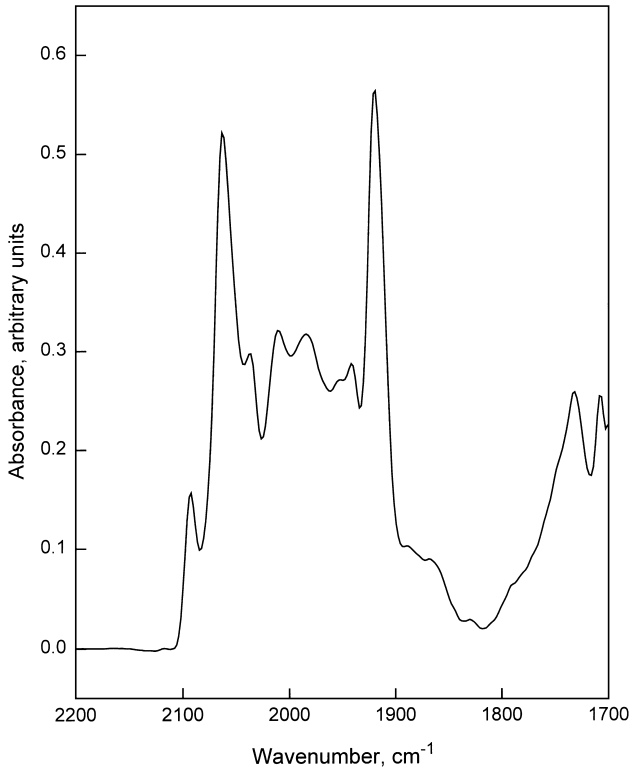

FIG. 2. Infrared spectrum of the species formed by treatment of adsorbed $[Ir(CO)_2(acac)]$ in KLTL zeolite in CO at 1 atm and 175°C for 10 h.

$[HIr_4(CO)_{11}]^-$ and $[Ir(CO)_4]^-$; the possibility that there were small amounts of other iridium carbonyl species cannot be ruled out.

EXAFS spectroscopy. The normalized EXAFS data characterizing the carbonylated iridium species supported in KLTL zeolite (Fig. 3A) were obtained from the average of the X-ray absorption spectra of six scans. The raw EXAFS data show oscillations up to k (the wavevector) equal to about 16 Å^{-1}.

TABLE 2

Infrared Spectra in the Carbonyl Stretching Region Characterizing Molecular Clusters and KLTL Zeolite-Supported Species Formed by Carbonylation of Adsorbed $[Ir(CO)_2(acac)]$ at 1 atm and 175°C

Sample	ν_{CO} (cm^{-1})	Ref.
$[Ir(CO)_2(acac)]$ adsorbed in KLTL zeolite, followed by treatment in CO at 1 atm and 175°C for 10 h	2093 m, 2063 s, 2037 m, 2011 m, 1985 m, 1941 m, 1920 s, 1732 m and 1708 m	This work
$[HIr_4(CO)_{11}]^-$ on partially hydroxylated MgO	2084 w, 2047 s, 2013 m, 1880 w	(10)
$[PPN][HIr_4(CO)_{11}]$ in CH_3OH	2030 sh, 2017 s, 1990 m, 1980 sh, 1812 w	(25)
$Na[Ir(CO)_4]$ in THF	2000 w, 1898 s, 1868 sh	(26)
$[PPN][Ir(CO)_4]$ in THF	1892 s	(25)

TABLE 3

EXAFS Results Characterizing Iridium Carbonyl Clusters Prepared from $[Ir(CO)_2(acac)]$ Supported in KLTL Zeolite after Treatment in CO at 175°C and 1 atm for 10 h

Shell[a]	Coordination number, N	Distance, r (Å)	$10^3 \times$ Debye–Waller factor, $\Delta\sigma^2$ (Å^2)	Inner potential correction, ΔE_0 (eV)	EXAFS reference
Ir–Ir	2.91	2.731	1.22	−1.20	Pt–Pt
Ir–CO					
Ir–O*	2.46	2.961	0.50	−0.25	Ir–O*
$Ir–C_t$	2.10	1.886	−3.22	−4.57	Ir–C
$Ir–C_b$	0.79	2.043	−5.33	0.50	Ir–C
$Ir–O_{support}$	2.09	2.477	12.00	−20.45	Pt–O
Ir–Al	0.57	1.507	3.71	10.59	Ir–Al

[a] The subscripts t and b refer to terminal and bridging, respectively.

The EXAFS data analysis was performed with the Koningsberger difference file technique (27, 28) and the XDAP data analysis software (29) on the unweighted raw EXAFS data in k space over the range $3.54 < k < 15.91$ Å^{-1} as well as in r space (r is the distance from the absorber Ir atom) over the range $0 < r < 4$ Å. The data analysis procedure is essentially the same as that stated elsewhere (14).

The structural parameters determined in the data fitting are summarized in Table 3. The number of parameters used to fit the data in this main-shell analysis is 24; the statistically justified number, n, calculated from the Nyquist theorem (30) ($n = 2\Delta k \Delta r/\pi + 1$, where $\Delta k = 12.37$ Å^{-1} and $\Delta r = 4$ Å), is approximately 32. Figures 3A and B show the goodness of fit; the raw data are compared with the fit in both k space and r space. The residual spectrum shown in Fig. 3C was determined by subtracting the sum of the Ir–Ir + Ir–$O_{support}$ + Ir–M contributions (where M is an unidentified metal, possibly K, Al, or Si) from the raw EXAFS data, giving evidence of the carbonyl ligands in the carbonylated iridium species. The residual spectrum representing the Ir–Ir contribution is shown in Fig. 3D. The Ir–M contribution was weak, and the data are not sufficient to identify M.

Characterization of Decarbonylated Iridium Clusters Supported in KLTL Zeolite

EXAFS spectroscopy. The normalized EXAFS data (Fig. 4A) characterizing the decarbonylated iridium clusters formed after treatment of the zeolite-supported iridium carbonyl clusters were obtained from the average of the X-ray absorption spectra of six scans. The raw EXAFS data show oscillations up to k equal to about 16 Å^{-1}.

The EXAFS data analysis was carried out by essentially the same procedure used for the carbonylated iridium species. The data fitting was performed on the unweighted raw EXAFS data in k space over the range $3.61 < k < 15.41$ Å^{-1} as well as in r space over the range $0 < r < 4$ Å.

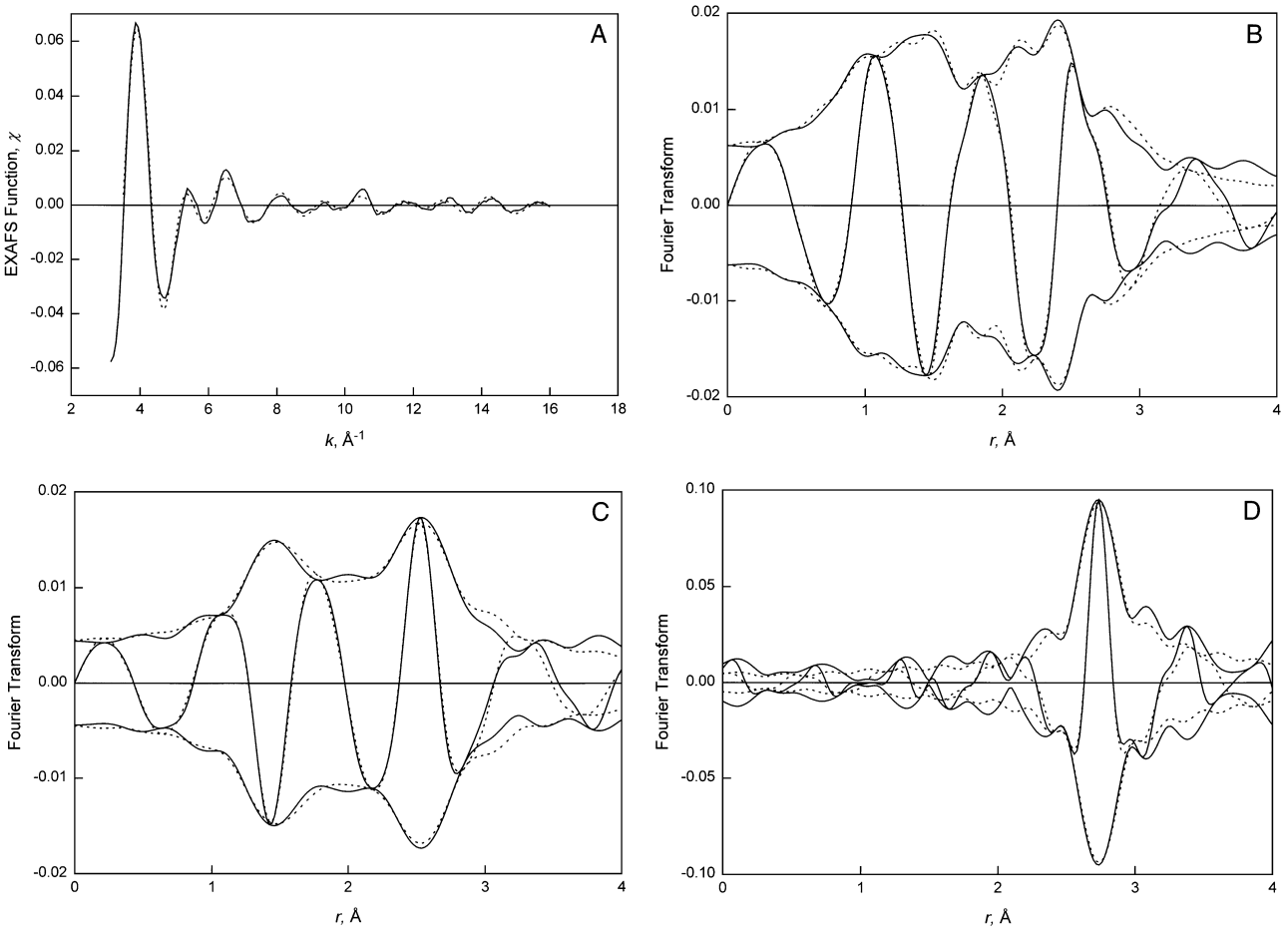

FIG. 3. Results of EXAFS data analysis characterizing the iridium carbonyl clusters formed by treatment of adsorbed [$Ir(CO)_2$(acac)] in KLTL zeolite in CO at 1 atm and 175°C for 10 h: (A) raw EXAFS function (solid line) and sum of the calculated Ir–Ir + Ir–C_t + Ir–C_b + Ir–O* + Ir–$O_{support}$ + Ir–M contributions (dashed line); (B) imaginary part and magnitude of Fourier transform (unweighted, $\Delta k = 3.54$–15.91 Å^{-1}) of raw EXAFS function and sum of the calculated Ir–Ir + Ir–C_t + Ir–C_b + Ir–O* + Ir–$O_{support}$ + Ir–M contributions (dashed line); (C) residual spectrum illustrating the contributions of carbonyl ligands: imaginary part and magnitude of Fourier transform (unweighted, $\Delta k = 3.54$–15.91 Å^{-1}) of raw EXAFS data minus calculated Ir–Ir + Ir–$O_{support}$ + Ir–M contributions (solid line) and calculated Ir–C_t + Ir–C_b + Ir–O* contributions (dashed line); (D) residual spectrum illustrating the Ir–Ir contribution: imaginary part and magnitude of Fourier transform (unweighted, $\Delta k = 3.54$–15.91 Å^{-1}) of raw EXAFS data minus calculated Ir–O* + Ir–C_t + Ir–C_b + Ir–$O_{support}$ + Ir–M contributions (solid line) and calculated Ir–Ir contribution (dashed line).

The results of the EXAFS analysis confirm the presence of Ir–Ir and Ir–support interactions; the latter include Ir–O_s and Ir–O_l contributions (where s and l refer to short and long, respectively); evidence of a weak contribution suggested to be Ir–M (where M is K, Al, or Si, but cannot be identified further) was also found. The structural parameters determined by the data fitting are summarized in Table 4. The number of parameters used in this main-shell analysis is 16; the statistically justified number, *n*, estimated from the Nyquist theorem (30), is approximately 32. Comparisons of the raw EXAFS data with the fits in *k* space and in *r* space are shown in Figs. 4A and B, respectively. The residual spectra giving evidence of the Ir–Ir, Ir–$O_{support}$, and Ir–M contributions are shown in Figs. 4C, D, and E, respectively.

A sample of KLTL zeolite-supported iridium carbonyl clusters was separately decarbonylated by treatment in He (rather than H_2) at 400°C for 2 h. The EXAFS data characterizing the decarbonylated iridium species indicate no significant contributions that could be ascribed to Ir–Ir interactions; rather, a significant Ir–O_s contribution was observed at a distance of about 2.0 Å. The results show that on removal of the carbonyl ligands from the metal frame during the treatment in He, the iridium clusters fragmented.

H_2 chemisorption. The difference between the two adsorption isotherms resulted in a H : Ir ratio of 0.62 for the catalyst that had been decarbonylated in H_2 at 400°C.

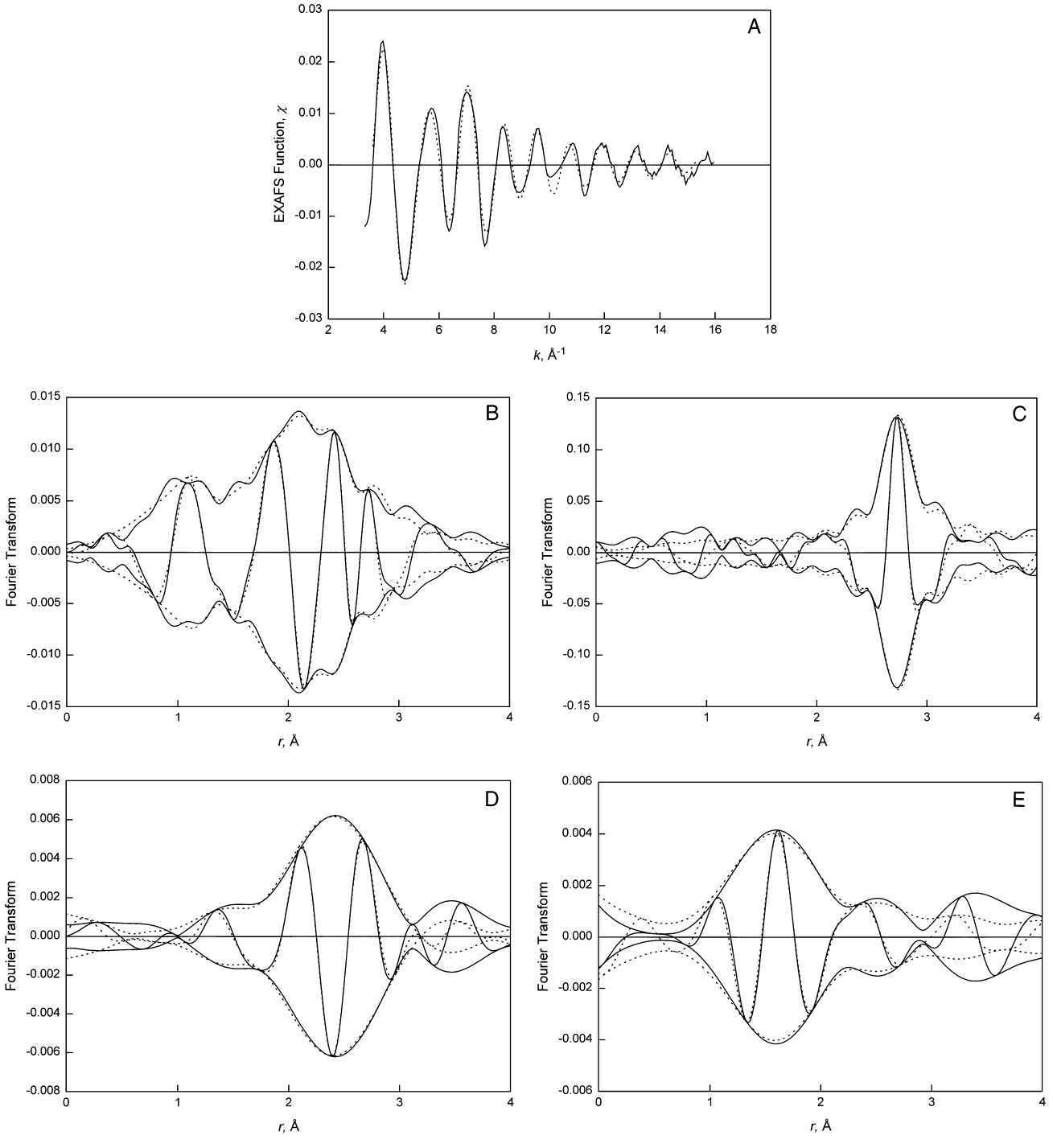

FIG. 4. Results of EXAFS analysis characterizing KLTL zeolite-supported iridium clusters formed by decarbonylation of KLTL zeolite-supported iridium carbonyl clusters in H_2 at 400°C for 2 h: (A) raw EXAFS function (solid line) and sum of the calculated Ir–Ir + Ir–O_s + Ir–O_l + Ir–M contributions (dashed line); (B) imaginary part and magnitude of Fourier transform (unweighted, $\Delta k = 3.61$–15.41 Å^{-1}) of raw EXAFS function (solid line) and sum of the calculated Ir–Ir + Ir–O_s + Ir–O_l + Ir–M contributions (dashed line); (C) residual spectrum illustrating the Ir–Ir contribution: imaginary part and magnitude of Fourier transform (unweighted, $\Delta k = 3.61$–15.41 Å^{-1}) of raw EXAFS data minus calculated Ir–O_s + Ir–O_l + Ir–M contributions (solid line) and calculated Ir–Ir contribution (dashed line); (D) residual spectrum illustrating the contributions of Ir–O interactions: imaginary part and magnitude of Fourier transform (unweighted, $\Delta k = 3.61$–8.0 Å^{-1}) of raw EXAFS data minus calculated Ir–Ir + Ir–M contributions (solid line) and calculated Ir–O_s + Ir–O_l contributions (dashed line); (E) residual spectrum illustrating the contributions of Ir–M contribution: imaginary part and magnitude of Fourier transform (unweighted, $\Delta k = 3.61$–8.0 Å^{-1}) of raw EXAFS data minus calculated Ir–Ir + Ir–O_s + Ir–O_l contributions (solid line) and calculated Ir–M contribution (dashed line).

TABLE 4

EXAFS Results Characterizing Iridium Clusters Formed by Decarbonylation of Iridium Carbonyl Clusters Supported in KLTL Zeolite in H_2 at 400°C

Shell	Coordination number, N	Distance, r (Å)	$10^3 \times$ Debye–Waller factor, $\Delta\sigma^2$ (Å^2)	Inner potential correction, ΔE_0 (eV)	EXAFS reference
Ir–Ir	4.17	2.727	1.03	−1.50	Pt–Pt
Ir–$O_{support}$					
Ir–O_s	0.97	2.171	1.96	−7.13	Pt–O
Ir–O_l	0.80	2.700	−7.10	−10.34	Pt–O
Ir–Al	0.46	1.543	4.62	13.54	Ir–Al

Toluene Hydrogenation Catalyzed by Iridium Clusters in KLTL Zeolite

Toluene hydrogenation was carried out with the catalyst formed by treatment of iridium carbonyl clusters supported in KLTL zeolite in H_2 at 400°C for 2 h, followed by purging with He for 0.5 h. The toluene conversions were differential, being less than 0.1%. [Plots of conversion versus inverse space velocity were found to be nearly linear at conversions less than 0.5% when the catalysts were iridium clusters on various supports (31–33).] The activity of the catalyst decreased about 30–40% during an initial induction period of about 1 h and then became almost time invariant. Thus, the conversions indicate nearly steady-state operation following the induction period. The rates, calculated from the conversions, are represented in units of moles of toluene converted (g of catalyst · s)$^{-1}$ (Fig. 5). The apparent activation energy determined from the temperature dependence of the reaction rates was found to be 6.0 kcal/mol.

The catalytic activity data for toluene hydrogenation catalyzed by the iridium clusters supported in KLTL zeolite are compared in Table 5 with those reported for Ir_6 on γ-Al_2O_3 and for iridium aggregates (Ir_{agg}) on γ-Al_2O_3, where the aggregates consisted of about 50 atoms each, on average, corresponding to a dispersion of about 70% (14). The catalytic activities are represented in Table 5 as turnover frequencies; the values characterizing each of the catalysts were estimated per surface atom, and the supported iridium clusters were assumed to be 100% dispersed on the support, with no account being taken of the possibility that some of the Ir atoms were inaccessible because of their interactions with the support. The data show that KLTL zeolite-supported iridium clusters have about the same activity as γ-Al_2O_3-supported Ir_6 clusters for toluene hydrogenation, but the activity is an order of magnitude less than that of Ir_{agg}/γ-Al_2O_3.

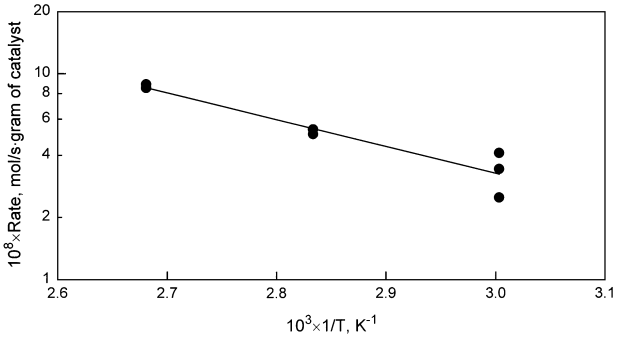

FIG. 5. Arrhenius plot for toluene hydrogenation catalyzed by KLTL zeolite-supported iridium clusters formed by decarbonylation of iridium carbonyl clusters in KLTL zeolite in H_2 at 400°C for 2 h. Reaction conditions: $P_{toluene} = 50$ Torr, $P_{H_2} = 710$ Torr; total feed flow rate: 46 ml/min (NTP); catalyst mass: 80 mg, 1 wt% Ir.

TABLE 5

Comparisons of Rates of Toluene Hydrogenation Catalyzed by Iridium Catalysts Supported in KLTL Zeolite and on γ-Al_2O_3 at $P_{toluene} = 50$ Torr and $P_{H_2} = 710$ Torr

Catalyst	Temperature (°C)	$10^3 \times$ TOF (molecules of toluene/Ir atom · s)[a]
Ir_6/KLTL[b,c]	60	0.6
	80	1.0
	100	1.7
Ir_6/γ-Al_2O_3[d]	60	1.7
	80	3.8
	100	7.3
Ir_{agg}/γ-Al_2O_3[e]	60	13.9
	80	25.3
	100	50.4

[a] TOF (turnover frequency) was calculated per surface Ir atom from catalytic reaction rate data. Rates are per total surface Ir atom, with no account taken of any effects of inaccessibility of Ir atoms associated with the support.

[b] The iridium clusters in KLTL zeolite have an average nuclearity of approximately 6, determined on the basis of the EXAFS results showing a first-shell Ir–Ir coordination number of about 4.

[c] Ir_6 was assumed to have 100% dispersion in KLTL zeolite.

[d] Ir_6 was assumed to have 100% dispersion on the surface of γ-Al_2O_3 (14).

[e] Iridium aggregates were about 70% dispersed on the surface, as estimated from the EXAFS data, assuming spherical particles (14).

Catalysis experiments were carried out under the same conditions with the supported iridium clusters formed after treatment of iridium carbonyl clusters supported in KLTL zeolite in H_2 at 400°C for 2 h but without purging with He at 400°C prior to the measurements. The rate data show that the activity of the catalyst pretreated under these conditions was less than 10% of that of the catalyst pretreated in H_2 followed by purging with He.

n-Hexane Reforming Catalyzed by Iridium Clusters in KLTL Zeolite

n-Hexane reforming catalysis was carried out with the Ir/KLTL zeolite formed by treatment of iridium carbonyl

TABLE 6

Selectivities in *n*-Hexane Conversion Catalyzed by Ir/KLTL Zeolite[a]

Reaction temperature (°C)	Selectivity				
	C_1	C_2–C_5	*i*-C_6	Benzene	Ultimate benzene
340[b]	0.196	0.458	0.142	0.205	0.238
380[c]	0.478	0.309	0.029	0.194	0.200

[a] Reaction conditions: 1 atm total pressure, H_2/*n*-hexane = 7 (molar).
[b] *n*-Hexane conversion was 35% at 340°C.
[c] *n*-Hexane conversion was 91% at 380°C.

clusters supported in KLTL zeolite in H_2 at 400°C for 2 h. At 340 and 380°C, the *n*-hexane conversions were about 35 and 91%, respectively; the products included C_1–C_5 hydrocarbons, methylcyclopentane, hexenes, and benzene.

Selectivity for benzene is defined (34) as the amount of *n*-hexane converted to benzene divided by the total amount of *n*-hexane converted. Because the products include other C_6 hydrocarbons that would also react to form benzene, a second definition of benzene selectivity, referred to as the ultimate benzene selectivity, is also used to account for the loss of C_6 hydrocarbons resulting from hydrogenolysis (34). The ultimate benzene selectivity is the mass of *n*-hexane converted to benzene divided by the mass of *n*-hexane converted to benzene plus light hydrocarbons (C_1–C_5). Selectivities for formation of the various products at 340 and 380°C are summarized in Table 6. The benzene selectivity was about 20% in each case.

At 420°C, *n*-hexane was 100% converted, with 99% of the *n*-hexane converted to C_1–C_3 hydrocarbons and 1% converted to benzene; there were no measurable C_4–C_6 hydrocarbons other than benzene in the products.

The Ir/KLTL zeolite was found to be a stable catalyst for *n*-hexane reforming (Fig. 6); it retained the same benzene selectivity at the same conversion during 40 h of continuous operation.

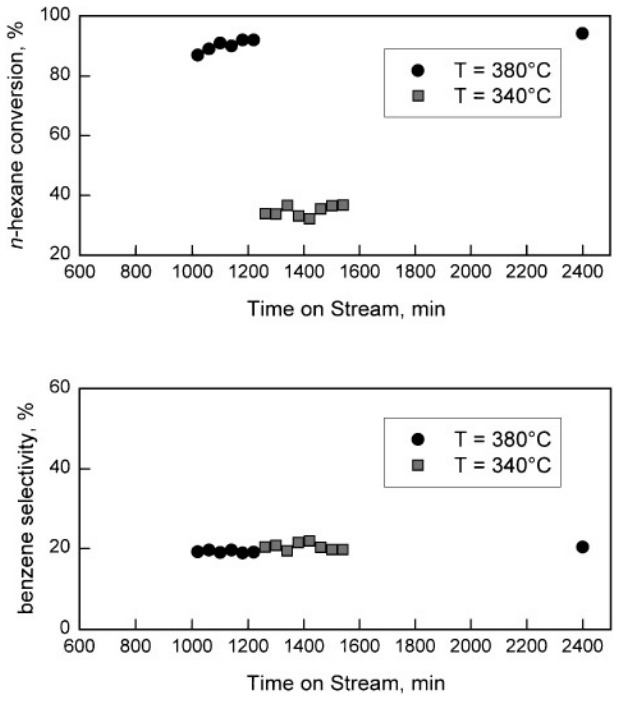

FIG. 6. *n*-Hexane dehydrocyclization catalyzed by KLTL zeolite-supported iridium clusters in a flow reactor: evidence of catalyst stability. Reaction conditions: $P_{n\text{-hexane}} = 95$ Torr, $P_{H_2} = 665$ Torr; total feed flow rate: 22 ml(NTP)/min; catalyst mass: 200 mg (1 wt% Ir).

DISCUSSION

Iridium Carbonyl Clusters in KLTL Zeolite

Infrared spectroscopy. The infrared spectrum characterizing the surface-bound iridium carbonyl species formed by treatment of the mononuclear iridium dicarbonyl precursor in KLTL zeolite indicates the formation of a mixture of iridium carbonyls, possibly including $[HIr_4(CO)_{11}]^-$; however, the shifts relative to those of this cluster anion are so large as to make the suggested assignment only tentative. If the suggested assignments are correct, then the shifts of the terminal ν_{CO} bands of $[HIr_4(CO)_{11}]^-$ and $[Ir(CO)_4]^-$ in KLTL zeolite to higher frequencies relative to those of $[HIr_4(CO)_{11}]^-$ and $[Ir(CO)_4]^-$ in solution (Table 2) can be interpreted as a consequence of electron withdrawal from the metal framework by surface cations such as Al^{3+} and Si^{4+}, resulting in decreased backbonding resulting from the interaction between the *d* orbital of the iridium atom and the antibonding orbital of the CO ligand.

The shifts of the bridging ν_{CO} bands of the clusters tentatively identified as $[HIr_4(CO)_{11}]^-$ in KLTL zeolite to lower frequencies (1732 and 1708 cm^{-1}) relative to those of $[HIr_4(CO)_{11}]^-$ in solution (1800 cm^{-1}, Table 2) are consistent with strong interactions of the oxygen atoms of the bridging CO ligands with surface cations (35), leading to weakened C–O bonding and decreased C–O stretching frequencies. The appearance of two bridging ν_{CO} bands (at 1732 and 1708 cm^{-1}) (instead of one) characterizing the surface-bound iridium species is suggested to be a result of interactions between the surface cations and the bridging CO ligands with different orientations (36).

Shifts of the terminal ν_{CO} bands to higher frequencies and of the bridging ν_{CO} bands to lower frequencies in the infrared spectra of supported metal carbonyl clusters have been reported by numerous investigators (17, 37), and such shifts have been interpreted (38, 39) as evidence of adduct formation, whereby, for example, CO ligands of $[(C_5H_5)Fe(CO)_2]_2$ interact with Lewis acids such as $Al(C_2H_5)_3$.

Adsorbed organometallic compounds have been used to probe properties of metal oxide surfaces, with the ν_{CO} shifts

of the adsorbed metal carbonyls being easily measured indicators of the strength of the bonding of the adsorbed species with surface cations (35, 40, 41). Relative to the ν_{CO} bands of $[HIr_4(CO)_{11}]^-$ adsorbed on partially dehydroxylated MgO (10), the terminal and bridging ν_{CO} bands of the clusters suggested to be $[HIr_4(CO)_{11}]^-$ in KLTL zeolite are shifted to higher frequencies and lower frequencies, respectively. These results suggest that cluster anions interact more strongly with the zeolite than with partially hydroxylated MgO.

EXAFS spectroscopy. The EXAFS data characterizing the iridium carbonyl clusters supported in KLTL zeolite show an average first-shell Ir–Ir coordination number of 2.9, indicating iridium carbonyl clusters having a (nearly) tetrahedral metal framework, consistent with the suggestion that the clusters are $[HIr_4(CO)_{11}]^-$.

The EXAFS results indicate a total Ir–C coordination number of 2.9 and an Ir–O* (O* refers to carbonyl oxygen) coordination number of 2.5. The apparent discrepancy indicated by the difference in the coordination numbers for C and O* has been explained (13) as a result of multiple scattering effects which lead to an underestimation of the Ir–O* coordination number for bridging CO ligands. On the basis of the more reliable Ir–C coordination number, we estimate that there were approximately three carbonyl ligands bonded to each iridium atom in the sample, on average. The suggested structural model is in close agreement with the structure of the anionic tetrairidium cluster, $[HIr_4(CO)_{11}]^-$, which, in the crystalline state, has a tetrahedral metal frame and 10 terminal and one bridging CO ligand per cluster (26); there are three carbonyl ligands associated with each iridium atom.

Therefore, on the basis of the EXAFS data, we infer that the product formed from the mononuclear iridium dicarbonyl precursor in KLTL zeolite was predominantly $[HIr_4(CO)_{11}]^-$; this result is consistent with the infrared data, which show that a small amount of $[Ir(CO)_4]^-$ was also present in the sample.

Surface-Mediated Synthesis of Iridium Carbonyl Clusters

Surface-mediated syntheses have been reported for a number of iridium carbonyl clusters (42). Neutral compounds, including $[Ir_4(CO)_{12}]$ and $[Ir_6(CO)_{16}]$, and anions, including $[HIr_4(CO)_{11}]^-$, $[Ir_6(CO)_{15}]^{2-}$, and $[Ir_8(CO)_{22}]^{2-}$, have been prepared from mononuclear iridium dicarbonyl precursors on various metal oxide and zeolite supports, including MgO (10, 25), γ-Al_2O_3 (11, 14, 41), NaY zeolite (15), and NaX zeolite (43). The synthesis chemistry on the surfaces parallels the solution chemistry of iridium carbonyl clusters, provided that the surfaces have acid–base properties comparable to those of the solutions (42).

KLTL zeolite is basic, and the basicity of this support is recognized as important in affecting the state and catalytic properties of the metal in the pores (34). Basic zeolites are media for the formation of anionic metal carbonyl clusters, including $[HIr_4(CO)_{11}]^-$ and $[Ir_6(CO)_{15}]^{2-}$ in NaX zeolite (43) and $[Pt_9(CO)_{18}]^{2-}$ and/or related platinum carbonyls in NaY zeolite and in some zeolite samples made basic by addition of alkali hydroxides (44–46). Synthesis of Chini–Longoni cluster anions (47), $[Pt_3(CO)_6]_n^{2-}$ in zeolite LTL was reported by Besoukhanova *et al.* (48). The structures of the platinum carbonyls in zeolite LTL, however, are less than well known; it is regarded as likely that mixtures were present in some of the reported samples (44). Mojet and Koningsberger (49) prepared platinum clusters (5–6 atoms in average nuclearity) from a salt precursor in KLTL zeolite that, on exposure to CO at room temperature, formed carbonylated species suggested on the basis of EXAFS data to be $[Pt(CO)_2]_3$ stabilized by the zeolite pore walls.

The present work is the first report of the preparation of iridium carbonyls in zeolite LTL. Treatment of iridium dicarbonyls in KLTL zeolite in CO at 175°C led to formation of $[HIr_4(CO)_{11}]^-$; in contrast, treatment of iridium dicarbonyls in NaX zeolite under the same conditions led to formation of $[Ir_6(CO)_{15}]^{2-}$ (43). The straight, narrow pores of KLTL zeolite could present steric limitations affecting the size of metal carbonyl clusters that can form in the pores; consistent with this statement, there is no evidence of the bulky $[Ir_8(CO)_{22}]^{2-}$ in any zeolite, although it forms on metal oxide surfaces (10).

The formation of $[Ir(CO)_4]^-$ along with $[HIr_4(CO)_{11}]^-$ in KLTL zeolite is indicative of the zeolite's strong basicity. The evidence of the need for strong basicity for the formation of this anion was reported by Angoletta *et al.* (26), who observed that $[Ir(CO)_4]^-$ formed in strongly basic solutions but not weakly basic solutions. Consistent with this chemistry, Kawi and Gates (25) inferred that $[Ir(CO)_4]^-$ formed as an intermediate in the surface reaction leading to $[HIr_4(CO)_{11}]^-$ on MgO; the results of the present work suggest that $[Ir(CO)_4]^-$ could have formed in KLTL as an intermediate as well; presumably, it was not completely converted into $[HIr_4(CO)_{11}]^-$. Much remains to be learned about KLTL zeolite as a synthesis medium for metal carbonyls, including identification of the source of hydrogen, which is suggested to be surface OH groups.

Preparation of Decarbonylated Iridium Clusters in KLTL Zeolite

Preparation of KLTL zeolite-supported iridium clusters with high dispersions has been reported by Triantafillou *et al.* (18, 19), who used an iridium salt precursor, $[Ir(NH_3)_5Cl]Cl_2$; the average iridium cluster size, determined by EXAFS spectroscopy, varied from about 7 to 20 Å, depending on the zeolite K : Al atomic ratio (which varied from 0.34 to 1.56). The data characterizing the iridium clusters in the sample with a K : Al atomic ratio of 1.08 indicate that the clusters were extremely small, with average nuclearities of 4–6 atoms.

In the present work, the K : Al ratio was also 1.08, and iridium clusters nearly as small as the smallest ones observed by Triantafillou *et al.* were prepared, now from organometallic precursors. The results of the EXAFS analysis reported here show a first-shell Ir–Ir coordination number of about 4 (Table 4), consistent with the presence of octahedral Ir_6 clusters in the zeolite pores. The lack of peaks in the Fourier transform corresponding to higher-shell Ir–Ir contributions indicates that there was no significant sintering of iridium to form larger clusters or crystallites inside or outside of the zeolite pores. Therefore, we infer that the clusters formed from the iridium carbonyl precursors in KLTL zeolite were nearly uniform and nearly molecular in character, having an average nuclearity of about 6.

The hydrogen chemisorption result indicates that the chemisorption on these small iridium clusters in KLTL zeolite is markedly less than that on (metallic) iridium particles (50). Triantafillou *et al.* (19) observed H : Ir ratios as low as 0.30 and 0.63 for KLTL zeolite-supported iridium clusters modeled as Ir_4 and Ir_6, formed by reducing the iridium salt precursors in H_2 at 300 and 500°C, respectively. The latter value is in good agreement with the value (0.62) reported here. Similar low H : Ir ratios have been observed for extremely small iridium clusters modeled as Ir_4 and formed by decarbonylation of $[HIr_4(CO)_{11}]^-$ supported on MgO (51).

Triantafillou *et al.* (18) had also reported an H : Ir ratio of 2.6 for KLTL zeolite-supported iridium clusters with nuclearities of about 4 and 6 atoms, respectively; however, these ratios resulted from measurements of only single adsorption isotherms representing both chemisorption and physisorption and, therefore, giving high values of the H : Ir ratios.

Triantafillou *et al.* (18) concluded on the basis of transmission electron microscopy that their 4- to 6-atom iridium clusters, formed by reduction of the salt precursor in H_2 at 500°C, were present predominantly in the zeolite pores. As there is no evidence of clusters larger than approximately 6-atom clusters in our samples, we suggest that they were also present predominantly in the zeolite pores.

Lack of Retention of Metal Framework of Iridium Carbonyl Clusters during Decarbonylation in KLTL Zeolite

Decarbonylation of supported tetrairidium or hexairidium carbonyl clusters with (near) retention of the metal frame has been reported to give Ir_4 and Ir_6 on MgO (10, 12, 13), Ir_4 and Ir_6 on γ-Al_2O_3 (11, 14), Ir_4 and Ir_6 in NaY zeolite (15, 52), and Ir_4 in NaX zeolite (53). These results demonstrate that there is some generality to the approach of preparing structurally well-defined metal clusters by decarbonylation of metal carbonyl precursors.

In the present work, the KLTL zeolite-supported iridium carbonyl clusters, predominantly $[HIr_4(CO)_{11}]^-$, were decarbonylated to give clusters that are approximated on the basis of the EXAFS data as Ir_6. Thus, we infer that the tetrairidium clusters were not simply decarbonylated, but instead were decarbonylated, possibly with slight aggregation to form a mixture of clusters that are represented, on average, as hexairidium clusters.

Catalytic Activity of KLTL-Supported Iridium Clusters for Toluene Hydrogenation

The catalytic activity of Ir/KLTL zeolite formed by treatment of iridium carbonyl clusters in KLTL zeolite in H_2 at 400°C is three to four times less than that of Ir_6/γ-Al_2O_3 for toluene hydrogenation and an order of magnitude less than that of Ir_{agg}/γ-Al_2O_3 (Table 5). The Ir_{agg}/γ-Al_2O_3 catalyst was a conventional supported metal catalyst, incorporating nonuniform particles of iridium that are regarded as large enough to be nearly metallic in character (32). Considering that the iridium clusters in KLTL have an average nuclearity of approximately 6, nearly the same as that of Ir_6/γ-Al_2O_3, we conclude that the catalytic properties of the supported iridium clusters and those of the supported iridium aggregates are significantly different from each other, with the catalytic activity of the clusters being markedly less than that of the aggregates. Similar results have been reported characterizing catalytic activities of supported iridium clusters, such as Ir_4 on γ-Al_2O_3 (33) and Ir_4 and Ir_6 on MgO (32); all of the supported clusters are less active for toluene hydrogenation than supported iridium catalysts with metallic character. It was also reported (54) that Ir_4/MgO is less active than Ir_{agg}/MgO for cyclohexene hydrogenation. Thus, all the data are consistent with the conclusion (32, 55) that the concept of structure insensitivity (56, 57) in metal catalysis, which has been shown to be valid for supported metals in the size range larger than about 10 Å, does not extend to smaller clusters such as Ir_4 and Ir_6 on metal oxide or zeolite supports. The causes of the deviation from the pattern of structure insensitivity are not yet elucidated (14, 32, 33).

A summary of the data allowing a comparison of the catalytic activities of supported iridium cluster catalysts (Table 7) shows that the activity increases in the order Ir_6/MgO < Ir_6/KLTL zeolite < Ir_6/γ-Al_2O_3. Likewise, Ir_4/MgO has been shown less active than Ir_4/γ-Al_2O_3 (Table 7). These data indicate a preliminary pattern of the support effects on the catalytic activity of iridium clusters. The effects are small, however, and more data are needed to elucidate their nature; in particular, the comparison stated here does not take account of differing degrees of hydroxylation of the supports.

The data show that the Ir/KLTL catalyst that had been pretreated in H_2 at 400°C but without purging with He at the same temperature is about 90% less active than the Ir/KLTL catalyst pretreated in H_2 followed by purging with He. The results suggest that hydrogen might have been strongly adsorbed on the Ir atoms during the pretreatment and might thus have inhibited the catalysis by hindering the

TABLE 7

Comparisons of Catalytic Activities of Supported Iridium Clusters and Supported Iridium Aggregates for Toluene Hydrogenation at Temperature = 60°C, $P_{toluene}$ = 50 Torr, and P_{H_2} = 710 Torr

Catalyst	$10^3 \times$ TOF (molecules of toluene/Ir atom · s)[a,b]	Ref.
Ir_4/MgO	0.63	(32)
Ir_4/γ-Al_2O_3	1.58	(33)
Ir_6/MgO	0.25	(32)
Ir_6/KLTL	0.64	This work
Ir_6/γ-Al_2O_3	1.72	(14)
Ir_{agg}/γ-Al_2O_3[c]	13.9	(14)

[a] TOF (turnover frequency) was calculated per surface Ir atom from catalytic reaction rate data. Rates are per total surface Ir atom, with no account taken of any effects of inaccessibility of Ir atoms associated with the support.

[b] Supported Ir_4 and Ir_6 clusters were assumed to have dispersions of 100%.

[c] Iridium aggregates were about 70% dispersed on the surface, estimated from the EXAFS data, assuming spherical particles (14).

adsorption of toluene molecules on the catalytic sites. Such an effect of hydrogen was also suggested by Xu *et al.* (32), who showed decreased toluene hydrogenation rates for Ir_4 and Ir_6 supported on MgO that had been treated in H_2 at 300°C relative to those measured for similar catalysts that had been pretreated only in He at 300°C. This suggestion, however, is in need of critical examination; there are too few data to rule out other possibilities, such as changes in the morphology of the iridium clusters resulting from the different treatments.

The apparent activation energy characterizing toluene hydrogenation catalyzed by Ir/KLTL zeolite was found to be 6.0 kcal/mol, which is approximately 50% lower than the value reported for toluene hydrogenation catalyzed by Ir_4 and Ir_6 clusters supported on γ-Al_2O_3, MgO, and NaY zeolite (14, 32, 33); this activation energy is also approximately 50% lower than the values reported for supported Ir, Pt, and Pd catalysts consisting of metallic particles on metal oxide supports (58, 59). Thus, we suggest that the catalytic activity of Ir/KLTL zeolite for toluene hydrogenation might have been influenced by transport of the reactants or products in the narrow pores of the KLTL zeolite. Consequently, the reaction rates reported for toluene hydrogenation may be less than the intrinsic rates.

Catalytic Performance of KLTL-Supported Iridium Clusters for n-Hexane Reforming

The Ir/KLTL catalyst was found to be low in selectivity for *n*-hexane aromatization to form benzene, as is typical of iridium catalysts; the selectivity for hydrogenolysis is correspondingly high. The results are qualitatively consistent with those reported by Triantafillou *et al.* (18, 19), who prepared their Ir/KLTL catalysts from salt precursors (in contrast to the organometallic precursor used in the present work); however, the conversions observed in this work were greater than most of those observed by Triantafillou *et al.* (18, 19), and so the comparison is inexact.

CONCLUSIONS

Iridium carbonyls, predominantly $[HIr_4(CO)_{11}]^-$ with a small amount of $[Ir(CO)_4]^-$, were formed in KLTL zeolite by treatment in CO at 175°C of mononuclear iridium dicarbonyls formed by adsorption of $[Ir(CO)_2(acac)]$. Decarbonylation of the supported iridium carbonyl by treatment in H_2 at 400°C resulted in clusters with an average nuclearity of about 6 atoms each, on average, as determined by EXAFS spectroscopy. The Ir/KLTL catalyst is active for toluene hydrogenation with turnover frequencies at 60 to 100°C slightly less than those observed for Ir_4 and Ir_6 clusters supported on MgO and on γ-Al_2O_3, but an order of magnitude less than those characterizing conventionally prepared supported iridium catalysts consisting of particles of about 50 atoms each, on average, which, in contrast to the clusters, are nearly metallic in character. The Ir/KLTL catalyst is also active for the reaction of *n*-hexane with H_2 at 340 to 420°C, but it is unselective for aromatization and selective for hydrogenolysis, as is typical of iridium generally.

ACKNOWLEDGMENTS

This research was supported by the U.S. Department of Energy, Office of Energy Research, Office of Basic Energy Sciences, Division of Chemical Sciences, Contract FG02-87ER13790. We thank the Stanford Synchrotron Radiation Laboratory, which is supported by the U.S. Department of Energy, for beam time. The equipment for adsorption measurements was purchased with support from a grant from the U.S. Department of Energy University Research Instrumentation Program. The EXAFS data were analyzed with the XDAP software (29).

REFERENCES

1. Bernard, J. R., *in* "Proceedings, 5th International Conference on Zeolites" (L. V. C. Rees, Ed.), p. 686. Heyden, London, 1980.
2. Tamm, P. W., Mohr, D. H., and Wilson, C. R., *in* "Catalysis 1987" (J. W. Ward, Ed.), p. 335. Elsevier, Amsterdam, 1988.
3. Hughes, T. R., Mohr, D. H., and Wilson, C. R., *in* "Proceedings, 7th International Conference on Zeolites" (Y. Murakami, A. Iijima, and J. W. Ward, Eds.), p. 725. Elsevier, Amsterdam/New York, 1986.
4. *Oil Gas J.* **190**, 29 (1992).
5. Rotman, D., *Chem. Week* **150**, 8 (1992).
6. Vaarkamp, M., Grondelle, J. V., Miller, J. T., Sajkowski, D. J., Modica, F. S., Lane, G. S., Gates, B. C., and Koningsberger, D. C., *Catal. Lett.* **6**, 369 (1990).
7. Vaarkamp, M., Modica, F. S., Miller, J. T., and Koningsberger, D. C., *J. Catal.* **144**, 611 (1993).
8. Miller, J. T., Meyers, B. L., Modica, F. S., Lane, G. S., Vaarkamp, M., and Koningsberger, D. C., *J. Catal.* **143**, 395 (1993).
9. Gates, B. C., *Chem. Rev.* **95**, 511 (1995).
10. Triantafillou, N. D., and Gates, B. C., *J. Phys. Chem.* **98**, 8431 (1994).

11. Kawi, S., Chang, J.-R., and Gates, B. C., *J. Phys. Chem.* **97**, 5375 (1993).
12. Van Zon, F. B. M., Maloney, S. D., Gates, B. C., and Koningsberger, D. C., *J. Am. Chem. Soc.* **115**, 10317 (1993).
13. Maloney, S. D., Kelley, M. J., Koningsberger, D. C., and Gates, B. C., *J. Phys. Chem.* **95**, 9406 (1991).
14. Zhao, A., and Gates, B. C., *J. Am. Chem. Soc.* **118**, 2458 (1996).
15. Kawi, S., Chang, J.-R., and Gates, B. C., *J. Am. Chem. Soc.* **115**, 4830 (1993).
16. Beutel, T., Kawi, S., Purnell, S. K., Knözinger, H., and Gates, B. C., *J. Phys. Chem.* **97**, 7284 (1993).
17. Lamb, H. H., Gates, B. C., and Knözinger, H., *Angew. Chem. Int. Ed. Engl.* **27**, 1127 (1988).
18. Triantafillou, N. D., Miller, J. T., and Gates, B. C., *J. Catal.* **155**, 131 (1995).
19. Triantafillou, N. D., Deutsch, S. E., Alexeev, O., Miller, J. T., and Gates, B. C., *J. Catal.* **159**, 14 (1996).
20. Jentoft, R. E., Deutsch, S. E., and Gates, B. C., *Rev. Sci. Instrum.* **67**, 2111 (1996).
21. Wyckoff, R. W. G. (Ed.), "Crystal Structures," 2nd ed., Vol. 1, p. 10. Wiley, New York, 1963.
22. Trömel, M., and Lupprich, E., *Z. Anorg. Chem.* **414**, 160 (1975).
23. Churchill, M. R., and Hutchinson, J. P., *Inorg. Chem.* **17**, 3528 (1978).
24. Lu, D., and Rehr, J. J., *J. Phys. (Paris) C8* **47**, 67 (1986).
25. Kawi, S., and Gates, B. C., *Inorg. Chem.* **31**, 2939 (1992).
26. Angoletta, M., Malatesta, L., and Caglio, G., *J. Organomet. Chem.* **94**, 99 (1975).
27. Van Zon, J. B. A. D., Koningsberger, D. C., van't Blik, H. F. J., and Sayers, D. E., *J. Chem. Phys.* **82**, 5742 (1985).
28. Kirlin, P. S., van Zon, F. B. M., Koningsberger, D. C., and Gates, B. C., *J. Phys. Chem.* **94**, 8439 (1990).
29. Vaarkamp, M., Linders, J. C., and Koningsberger, D. C., *Physica B* **209**, 159 (1995).
30. Crozier, E. D., Rehr, J. J., and Ingalls, R., *in* "X-ray Absorption: Principles, Applications, Techniques of EXAFS, SEXAFS, and XANES" (D. C. Koningsberger and R. Prins, Eds.), p. 395. Wiley, New York, 1988.
31. Xu, Z., Ph.D. thesis, University of Delaware, 1995.
32. Xu, Z., Xiao, F.-S., Purnell, S. K., Alexeev, O., Kawi, S., Deutsch, S. E., and Gates, B. C., *Nature (London)* **372**, 346 (1994).
33. Zhao, A., and Gates, B. C., *J. Catal.*, in press.
34. Lane, G. S., Modica, F. S., and Miller, J. T., *J. Catal.* **129**, 145 (1991).
35. Otten, M. M., and Lamb, H. H., *J. Am. Chem. Soc.* **116**, 1372 (1994).
36. Gladfelter, W. L., personal communication, 1991.
37. Rao, L.-F., Fukuoka, A., Kosugi, N., Kuroda, H., and Ichikawa, M., *J. Phys. Chem.* **94**, 5317 (1990).
38. Shriver, D. F., *J. Organomet. Chem.* **94**, 259 (1975).
39. Horwitz, C. P., and Shriver, D. F., *Adv. Organomet. Chem.* **23**, 219 (1984).
40. Gates, B. C., and Lamb, H. H., *J. Mol. Catal.* **52**, 1 (1989).
41. Zhao, A., and Gates, B. C., *Langmuir*, submitted.
42. Gates, B. C., *J. Mol. Catal.* **86**, 95 (1994).
43. Kawi, S., Chang, J.-R., and Gates, B. C., *J. Catal.* **142**, 585 (1993).
44. Chang, J.-R., Xu, Z., Purnell, S. K., and Gates, B. C., *J. Mol. Catal.* **80**, 49 (1993).
45. Li, G. J., Fujimoto, T., Fukuoka, A., and Ichikawa, M., *J. Chem. Soc. Chem. Commun.*, 1337 (1991).
46. Li, G. J., Fujimoto, T., Fukuoka, A., and Ichikawa, M., *Catal. Lett.* **12**, 171 (1992).
47. Longoni, G., and Chini, P., *J. Am. Chem. Soc.* **98**, 7225 (1976).
48. Besoukhanova, C., Guidot, J., Barthomeuf, D., Breysse, M., and Bernard, J. R., *J. Chem. Soc. Faraday Trans.* **77**, 1595 (1981).
49. Mojet, B. L., and Koningsberger, D. C., *Catal. Lett.* **39**, 191 (1996).
50. McVicker, G. B., Baker, R. T. K., Garten, R. L., and Kugler, E. L., *J. Catal.* **65**, 207 (1980).
51. Xiao, F.-S., Xu, Z., Alexeev, O., and Gates, B. C., *J. Phys. Chem.* **99**, 1548 (1995).
52. Kawi, S., Chang, J.-R., and Gates, B. C., *J. Phys. Chem.* **97**, 10599 (1993).
53. Kawi, S., and Gates, B. C., *J. Phys. Chem.* **99**, 8824 (1995).
54. Xu, Z., and Gates, B. C., *J. Catal.* **154**, 335 (1995).
55. Xiao, F.-S., Weber, W. A., Alexeev, O., and Gates, B. C., *in* "Proceedings of the 11th International Congress on Catalysis" (J. W. Hightower, W. N. Delgass, E. Iglesia, and A. T. Bell, Eds.), p. 1135. Elsevier, Amsterdam, 1996.
56. Boudart, M., *J. Mol. Catal.* **30**, 27 (1985).
57. Boudart, M., and Djéga-Mariadassou, G., "Kinetics of Heterogeneous Catalytic Reaction." Princeton Univ. Press, Princeton, NJ, 1984.
58. Lin, S. D., and Vannice, M. A., *J. Catal.* **143**, 554 (1993).
59. Rahaman, M. V., and Vannice, M. A., *J. Catal.* **127**, 251 (1991).